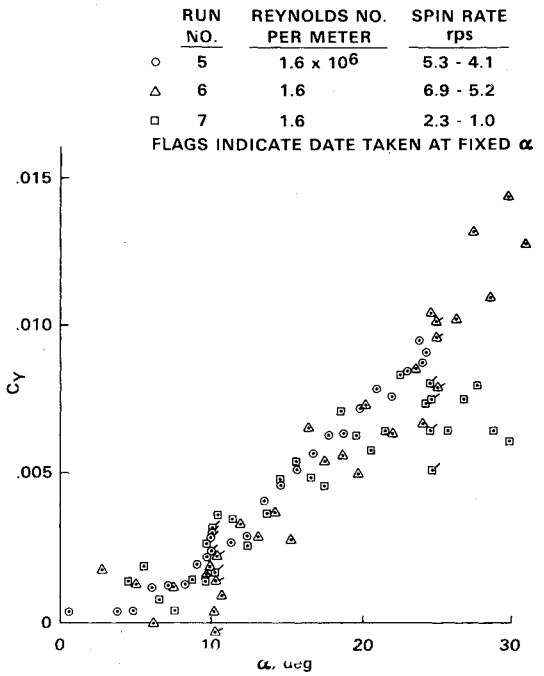

Fig. 4 Comparison of side force data with ablation at different spin rates.

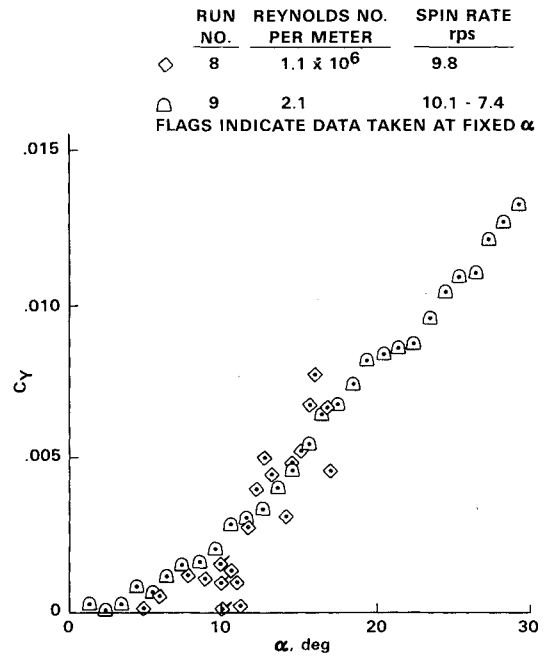

Fig. 5 Comparison of side force data with ablation at different Reynolds numbers.

A comparison of data from the nonablating model tests with data from one of the ablating model tests is shown in Fig. 3 and a significant side force due to ablation is clearly indicated. The ablating model data also indicate that the side force is a strong function of the angle of attack—nonlinear up to about 10 deg and linear at higher angles. In Fig. 4, data from three tests made with ablating models at different spin rates are compared. No significant effect of spin rate is seen over most of the angle-of-attack range; although above 25 deg angle of attack the side force data for spin rates between 1 and 2.3 rps are significantly lower than the data taken at higher spin rates. Thus, for camphor ablation at the test conditions reported here, the side force due to ablation was independent of spin rate at speeds greater than 1-2 rps for angles of attack up to 25 deg. In Fig. 5, data from two tests made at different Reynolds numbers are compared and show no significant effect of Reynolds number over the range investigated. It should be noted that completely laminar boundary layers are expected over the entire range of test conditions available in the Hypervelocity Research Tunnel.

The data show the angle-of-attack behavior of the side force due to ablation to be very similar to that of the normal force, and the magnitude of the side force to be roughly 1% of the normal force. The response of the camphor ablation to changes in angle of attack was evidently quite rapid since the data taken at fixed angles of attack do not indicate any large lag effects. The data for spin rates of 1-2.3 rps definitely follow a different trend beyond 25 deg but it is not clear whether this indicates a lag effect or is due to the low spin rate.

In the wind tunnel, positive angle of attack was nose-up and the direction of spin was clockwise, looking upstream. The direction of the observed side force was to the right, looking upstream, which is in agreement with the qualitative mechanism for the ablation-induced side force previously mentioned.

The center of pressure of the side force was also measured but due to the fact that the force was very small, accurate results were not obtained. In general, the experimental data indicate the side force center of pressure to be located 50-60% of the body length from the nosetip and independent of the angle of attack.

Normal force and pitch center of pressure measurements were also made and the results for the ablating models were in good agreement with those for the nonablating models. The normal force data were in good agreement with classical Newtonian flow theory. The center of pressure data for the ablating models showed small shifts ($< 1/2\%$ of body length), while the angle of attack was held constant at 10 and 25 deg. These shifts are believed to be due to the effect of shape change.

References

[1] Waterfall, A. P., "Effect of Ablation on the Dynamics of Spinning Re-Entry Vehicles," *Journal of Spacecraft and Rockets*, Vol. 6, Sept. 1969, pp. 1038-1044.

[2] Vaughn, H. R. and Reiss, G. E., "A Magnus Theory," *AIAA Journal*, Vol. 11, Oct. 1973, pp. 1396-1403.

Mixing of a Transverse Jet with a High Mach Number Stream

R. Rosen* and D. W. Harvey†
McDonnell Douglas Astronautics Company, Huntington Beach, Calif.

Nomenclature

c, γ = mass and molar concentration, respectively
c_{crit} = fraction of injectant within γ_{min} ellipse
g = ratio of x and y dimensions of γ_{min} ellipse
M = ratio of molecular weights of injectant to freestream
M_j = molecular weight of injectant

Presented as Paper 78-27 at the AIAA 16th Aerospace Sciences Meeting, Huntsville, Ala., submitted Feb. 13, 1978; revision received May 4, 1978. Copyright © American Institute of Aeronautics and Astronautics, Inc., 1978. All rights reserved.

Index categories: Supersonic and Hypersonic Flow; Airbreathing Propulsion.

*Senior Engineer/Scientist.
†Senior Engineer/Scientist. Member AIAA.

$\dot{m}$ = mass flux
$\bar{R}$ = universal gas constant
x = coordinate normal to plate measured from the half-shock point
x_{max} = height of Gaussian cutoff in x-z plane
z = downstream distance

Introduction

THE turbulent mixing of a transverse jet injected into a high Mach number stream is not well characterized, especially near the injector where the jet is turned downstream. Both analytical and experimental approaches to this problem have met with major difficulties. When information on such mixing is needed, as in calculating fuel rich jet interaction performance, low Mach number injectant concentration data,[1,2] fit by analytical expressions and extended to the higher Mach numbers of interest by a Mach number-dependent scale length,[3] are used.

This approach, however, encounters both practical and conceptual problems. The nature of the diffusion equation and the shape of the data suggest the use of circular or elliptical Gaussian concentration profiles in the data-fitting procedure. But a basic difficulty lies in the inability of the Gaussian, or, in fact, of any one-parameter profile using the assumption of geometric similarity, to include the potential core of the jet when it is necessary to do so.

This Note uses an indirect approach which omits consideration of the physics of mixing, but which is controlled by continuity and the shape of the jet shock. We assume the jet concentration profile, upstream of the point at which the potential core vanishes, to be Gaussian with a uniform core of pure injectant. The cross-sectional shape of the core is elliptical with all other concentrations existing on ellipses concentric about the half-shock point $\tilde{x}_{hs}$ (Fig. 1). The Gaussian is assumed to be cut off at a point such that a constant fraction (near 1) of the total jet flow is included. The profile shape and the core eccentricity are found from the condition that all the jet flow, and all the external flow intercepted by the jet shock, must be contained beneath that shock. This approach rests upon the fact that the jet shock shape is reasonably well known.[3,4] The result has the advantages that the assumed profile is physically reasonable and that it merges smoothly, at the point where the potential core vanishes, with the existing expressions, which are assumed valid downstream of this point.

Despite questions which may arise from the chosen assumptions, the present method supplies the only presently available answer to a real need for information on high Mach number mixing of a transverse jet.

Analysis and Results

The assumed concentration profile can be written as

$$c = \exp\left\{-\frac{1}{\eta}\left[\left(\frac{x}{x_1}\right)^2+\left(\frac{y}{y_1}\right)^2-1\right]\right\}$$

$$\text{for } (x,y) \text{ such that } \left(\frac{x}{x_1}\right)^2+\left(\frac{y}{y_1}\right)^2 \geq 1 \tag{1a}$$

and

$$c=1 \text{ for } (x,y) \text{ such that } \left(\frac{x}{x_1}\right)^2+\left(\frac{y}{y_1}\right)^2 \leq 1 \tag{1b}$$

where η is the $1/e$ half-width of the Gaussian, $\tilde{x}$ and $\tilde{x}_1$ are shown in Fig. 1, and all are functions of the downstream distance z. All lengths are nondimensionalized by h, the scale length.[3] The difference between the tilde and nontilde variables are that the latter have the half-shock point $(\tilde{x}_{hs},0)$ as their origin.

The Gaussian shape implies that injectant exists outside the jet shock. This is probably not the case in supersonic flow.

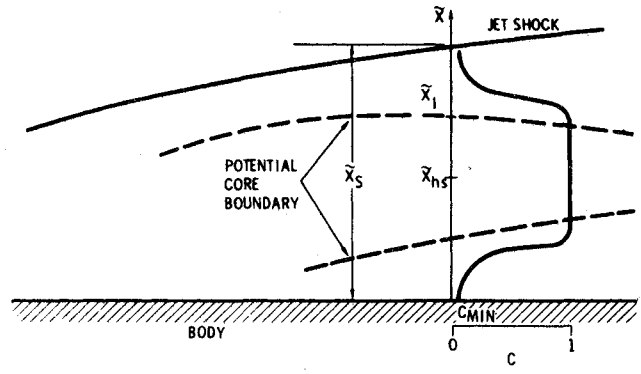

Fig. 1 Postulated concentration profile.

The assumption is therefore made that the Gaussian is cut off so that it does not extend to infinity in the radial direction; this implies that only a fraction c_{crit}, assumed fixed, of the injectant mass flow remains within the shock envelope.

The width scale of the Gaussian η can be obtained in terms of the minimum molar concentration γ which occurs at the point $(x_s,0)$:

$$\eta = \left\{1-\left(\frac{\tilde{x}_{hs}}{x_1}\right)^2\right\} \Big/ \ell n \left\{\frac{M\gamma_{min}}{1-(1-M)\gamma_{min}}\right\} \tag{2}$$

The total mass injected can be found after some algebra as

$$\dot{m}_j = \frac{\pi h^2}{g} M_j \frac{pu}{\bar{R}T}\left\{x_1^2+\frac{1}{1-M}(\tilde{x}_{hs}^2-x_1^2)\right.$$

$$\left.\times\left[\ell n\, M \Big/ \ell n \frac{M\gamma_{min}}{1-(1-M)\gamma_{min}}\right]\right\} \tag{3}$$

where for purposes of simplicity, the velocity u, as well as the pressure p, and temperature T at a fixed z are assumed independent of position. Only the density ρ is allowed to be a function of x and y, due solely to the variation in concentration of this mixture of perfect gases.

An expression for c_{crit} can be found by integrating the injected mass over the γ_{min} ellipse and dividing by $\dot{m}_j$:

$$c_{crit} = \left[F_1+F_2 \ell n \frac{1-(1-M)\gamma_{min}}{M}\right] \Big/ \left[F_1-F_2 \ell n\, M\right] \tag{4}$$

where

$$F_1 = x_1 \ell n \frac{M\gamma_{min}}{1-(1-M)\gamma_{min}} \tag{5}$$

$$F_2 = \frac{1}{1-M}[x_1^2-\tilde{x}_{hs}^2] \tag{6}$$

The final relation is obtained by summing the injected mass and freestream air captured within the shock envelope. This yields

$$1 = \frac{\rho_1 u_1}{\rho_\infty u_\infty}\left(1-\frac{1}{2g}\right)+\frac{2}{\pi \tilde{x}_s^2}\frac{\dot{m}_j}{\rho_\infty u_\infty}\left(\frac{\dot{m}_t}{\dot{m}_j}-1\right) \tag{7}$$

in which

$$\frac{\dot{m}_t}{\dot{m}_j} = \frac{F_1-[(1-M)/M]F_2 \ell n\, \gamma_{min}}{F_1-F_2 \ell n\, M} \tag{8}$$

Equations (2-4), (7), and (8) allow determination of the concentration profile.

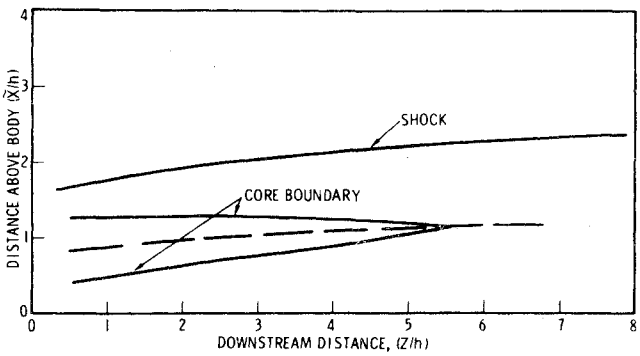

Fig. 2 Illustration of the decay of the core.

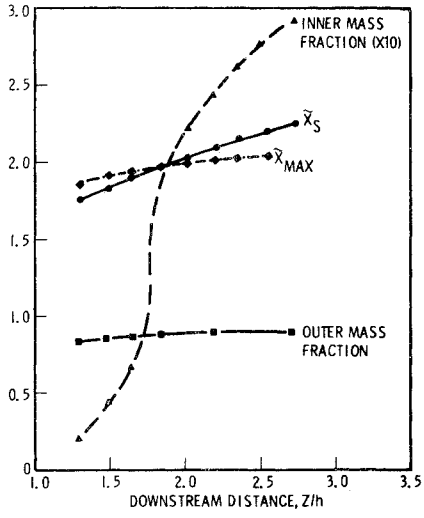

Fig. 3 Mass fractions of air and comparison of shock height and $\tilde{x}_{max}$ downstream of injection.

Figure 2 shows results of a typical high Mach number calculation, with the shock location and the upper and lower core boundaries centered about the half-shock height line. At about 5.5 scale lengths downstream of the injection point, the core vanishes and transition to the Gaussian profile occurs.

Other results for the conditions associated with a 6 deg cone at -5 deg angle of attack, 90,000 ft, and $M_\infty = 15$ are shown in Fig. 3. Comparisons of $\tilde{x}_s$ and $\tilde{x}_{max}$, the $\tilde{x}$ value corresponding to γ_{min} and $\tilde{y} = 0$ calculated from the Gaussian profiles, are given as a function of z. It can be seen that for the first three steps $\tilde{x}_{max}$ is greater than $\tilde{x}_s$, implying the existence of a uniform core. Further downstream $\tilde{x}_{max} < \tilde{x}_s$, implying no potential core remains. Also plotted on the figure are the mass fraction of air in the innermost and outermost of the three radial zones used in the calculation. It can be seen in the upstream region where the core exists that the flow is composed almost entirely of injectant. It is only due to the coarseness of the zones that any air is in the innermost zone. In the vicinity of the core disappearance, the mass fraction of air rises dramatically, signifying the introduction of air into the innermost zone at the end of the injectant core. Rapid changes do not occur in the outer zone when the injectant core vanishes, since there is already considerable mixing.

Remarks and Conclusions

Several aspects of the method just outlined should be noted. The results represent the upper limit on the amount of mixing in any given situation. Less mixing can occur without injectant appearing beyond the shock, but not more.

It may well be found, when experimental data are made available at sufficiently high Mach numbers, that the upper limit of mixing, as found by the method presented here, is the amount that actually occurs. If so, one might conjecture that a change in the physics of the mixing process would affect the shock location; for example, if a large increase in the rate of mixing were to occur, the shock would be required to shift outward to accommodate the wider concentration profiles. A possible mechanism for such a change in the mixing rate is the transition from laminar to turbulent mixing. This would then imply that turbulent-jet shocks would differ—would lie farther from the plate—compared to shocks about laminar transverse jets. This is a point for experimentalists to keep in mind.

The requirement that the profile cutoff be equal to the shock height in the x-z plane, rather than leaving room for an injectant-free shock layer there, may be viewed as somewhat arbitrary. It is true that a shock layer is likely to exist at every point beneath the shock, but secondary flows in both the jet and the shock layer will decrease the shock layer thickness in the x-z plane while increasing it elsewhere. Thus, the error involved is not large, and may, in any case, be limited to the extreme case of a nearly square profile.

Acknowledgment

This work was done under contract to BMDATC, Huntsville, Ala. The contract monitor was R. Riviere.

References

[1] Spaid, F. W., Zukoski, E. E., and Rosen, R., "A Study of Secondary Injection of Gases Into a Supersonic Flow," JPL TR 32-834, Aug. 1966.

[2] Orth, R. C. and Funk, J. A., "An Experimental and Comparative Study of Jet Penetration in Supersonic Flow," *Journal of Spacecraft & Rockets*, Vol. 4, Sept. 1967, pp. 1236-1242.

[3] Kallis, J. M., "Equivalent Solid Obstacle for Gas Injection Into a Supersonic Stream," *AIAA Journal*, Vol. 10, Oct. 1972, pp. 1342-1343.

[4] Harvey, D. W., Hopkins, D. F., and Rosen, R., "Experiments on Reacting Gas Jet Penetration," *AIAA Journal*, Vol. 15, Jan. 1977, pp. 76-82.

Navier-Stokes Solutions Using Stetter's Method

Randolph A. Graves, Jr.*
NASA Langley Research Center, Hampton, Va.
and
Noreen E. Johnson†
Spelman College, Atlanta, Ga.

Nomenclature

A = area
c = speed of sound
E = total internal energy
F = arbitrary function vector, see Eq. (4)
g = arbitrary function
k = thermal conductivity
N = total number of time steps to convergence
p = pressure
R = time step factor, see Eq. (6)
t = time
T = temperature
u = velocity
U = function vector, see Eq. (4)

Submitted Jan. 30, 1978; revision received April 27, 1978.
Index category: Computational Methods.
*Research Leader, Aerothermodynamics Branch. Member AIAA.
†Student.